Tryptophan 207 is crucial to the unique properties of the human voltage-gated proton channel, hH_V1

Vladimir V. Cherny,[1] Deri Morgan,[1] Boris Musset,[2] Gustavo Chaves[2], Susan M.E. Smith,[3] and Thomas E. DeCoursey[1]

[1]Department of Molecular Biophysics and Physiology, Rush University, Chicago, IL 60612
[2]Institute of Complex Systems 4 Zelluläre Biophysik, Forschungszentrum Jülich, 52425 Jülich, Germany
[3]Department of Molecular and Cellular Biology, Kennesaw State University, Kennesaw, GA 30144

Part of the "signature sequence" that defines the voltage-gated proton channel (H_V1) is a tryptophan residue adjacent to the second Arg in the S4 transmembrane helix: RxWRxxR, which is perfectly conserved in all high confidence H_V1 genes. Replacing Trp^{207} in human H_V1 (hH_V1) with Ala, Ser, or Phe facilitated gating, accelerating channel opening by 100-fold, and closing by 30-fold. Mutant channels opened at more negative voltages than wild-type (WT) channels, indicating that in WT channels, Trp favors a closed state. The Arrhenius activation energy, E_a, for channel opening decreased to 22 kcal/mol from 30–38 kcal/mol for WT, confirming that Trp^{207} establishes the major energy barrier between closed and open hH_V1. Cation–π interaction between Trp^{207} and Arg^{211} evidently latches the channel closed. Trp^{207} mutants lost proton selectivity at pH_o >8.0. Finally, gating that depends on the transmembrane pH gradient (ΔpH-dependent gating), a universal feature of H_V1 that is essential to its biological functions, was compromised. In the WT hH_V1, ΔpH-dependent gating is shown to saturate above pH_i or pH_o 8, consistent with a single pH sensor with alternating access to internal and external solutions. However, saturation occurred independently of ΔpH, indicating the existence of distinct internal and external pH sensors. In Trp^{207} mutants, ΔpH-dependent gating saturated at lower pH_o but not at lower pH_i. That Trp^{207} mutation selectively alters pH_o sensing further supports the existence of distinct internal and external pH sensors. Analogous mutations in H_V1 from the unicellular species *Karlodinium veneficum* and *Emiliania huxleyi* produced generally similar consequences. Saturation of ΔpH-dependent gating occurred at the same pH_o and pH_i in H_V1 of all three species, suggesting that the same or similar group(s) is involved in pH sensing. Therefore, Trp enables four characteristic properties: slow channel opening, highly temperature-dependent gating kinetics, proton selectivity, and ΔpH-dependent gating.

INTRODUCTION

Voltage-gated proton channels (H_V1) exist in diverse organisms ranging from unicellular marine species (Smith et al., 2011; Taylor et al., 2011) to humans (Ramsey et al., 2006). Their functions are equally diverse: conversion of CO_2 to calcite in coccolithophores (Taylor et al., 2011), triggering the bioluminescent flash in dinoflagellates (Smith et al., 2011), and in humans participating in innate immunity (DeCoursey, 2010), B cell signaling (Capasso et al., 2010), airway acid secretion (Iovannisci et al., 2010), histamine secretion (Musset et al., 2008b), sperm motility (Musset et al., 2012) and capacitation (Lishko et al., 2010), brain damage in ischemic stroke (Wu et al., 2012), breast cancer (Wang et al., 2012), and chronic lymphocytic leukemia (Hondares et al., 2014). All known and suspected H_V1 to date, even in species with just 15–18% sequence identity to the human H_V1 (hH_V1), share a perfectly conserved tryptophan (Trp^{207} in hH_V1) adjacent to the second of three Arg residues in the S4 transmembrane segment (Fig. S1) (DeCoursey, 2013). This Trp is part of the proposed signature sequence of the proton channel RxWRxxR (Smith et al., 2011), and is present even in several unconfirmed H_V1-like sequences in fungi in which the third Arg in S4 is replaced by Lys (e.g., *Fusarium oxysporum*, *Ophiostoma piceae*, and *Metarhizium anisopliae*). Among molecules that contain voltage-sensing domains (VSDs), only H_V1 and c15orf27 (whose function is unknown) contain Trp in this location (Smith et al., 2011). Here, we ask why this Trp has been conserved. We find that replacing Trp modifies four characteristic properties of hH_V1, revealing that it is central to the unique defining properties and functions of H_V1. Trp mutants opened and closed 30–100 times faster than WT, with gating kinetics less profoundly sensitive to temperature; they lost proton selectivity at high pH_o; and the unique ΔpH dependence of gating was compromised. The striking

Correspondence to Thomas E. DeCoursey: tdecours@rush.edu

Abbreviations used in this paper: CiVSP, *Ciona intestinalis* voltage-sensing phosphatase; hH_V1, human voltage-gated proton channel; H_V1, voltage-gated proton channel; VSD, voltage-sensing domain.

The Rockefeller University Press $30.00
J. Gen. Physiol. Vol. 146 No. 5 343–356
www.jgp.org/cgi/doi/10.1085/jgp.201511456

diversity of the effects of Trp mutation indicates that this residue plays a pivotal role in the H_V1 protein.

Tryptophan is the rarest amino acid in proteins, and in membrane proteins, it is often found close to lipid head groups, preferring the interfacial environment (Killian and von Heijne, 2000; MacCallum et al., 2008). Thus, the absolute conservation of a Trp in the middle of the S4 transmembrane segment of H_V1 requires some explanation. Three other Trp residues in hH_V1 are all in the intracellular N terminus. Perhaps because both Trp and Arg residues share ambivalence by exhibiting hydrophobic mixed with polar characteristics, they interact strongly with each other (Santiveri and Jiménez, 2010). In β-hairpin peptides and in other proteins, the guanidinium group of Arg stacks against the aromatic ring of Trp via cation–π (Gallivan and Dougherty, 1999) and van der Waals interactions, stabilizing the protein structure (Tatko and Waters, 2003; Santiveri and Jiménez, 2010). The proximity of Trp^{203} and R3 (the third Arg in the S4 segment, Arg^{207} in mouse) in the closed structure of the mouse H_V1 (mH_V1; Takeshita et al., 2014) appears to be consistent with this type of interaction, with amino-aromatic distances <6.0 Å (Burley and Petsko, 1986). In the structure identified as a closed conformation of mH_V1 (Takeshita et al., 2014), the indole side chain of Trp^{203} is directed away from the pore toward the interior of the lipid bilayer, pointing downward, partially shielding the R3 side chain, which is directed down and between S4 and S3 but also has some lipid exposure. In all open-state models (Ramsey et al., 2010; Wood et al., 2012; Kulleperuma et al., 2013; Chamberlin et al., 2014), all three Arg residues of the S4 segment face the pore, but Trp still faces away from the pore. We propose that Trp stabilizes the closed hH_V1 through cation–π interaction with Arg^{211}, and that loss of this stabilization contributes to the consequences of its mutation. A striking result was that whether Trp was replaced by Ala (hydrophobic), Ser (hydrophilic), or Phe (aromatic), H_V1 properties were changed by a quantitatively indistinguishable extent. This result suggests that the heterocyclic aromatic side chain of Trp uniquely anchors the S4 segment in the membrane.

MATERIALS AND METHODS

Gene expression

Site-directed mutants were created using the QuikChange (Agilent Technologies) procedure according to the manufacturer's instructions. Transfection was done as described previously (Kulleperuma et al., 2013). Both HEK-293 cells and COS-7 cells were used as expression systems. We showed previously that the properties of H_V1 expressed in both cell lines were indistinguishable (Musset et al., 2008a). No other voltage- or time-dependent conductances were observed under the conditions of this study. Although most mutations on hH_V1 were introduced into a Zn^{2+}-insensitive background (H140A/H193A), which we have done previously as a control for endogenous H_V1 (Musset et al., 2011), the level of expression of all mutants studied here was sufficiently high that contamination by native H_V1 was negligible.

Electrophysiology

In most experiments, cells expressing green fluorescent protein (GFP)-tagged proton channels were identified using inverted microscopes (Nikon) with fluorescence capability. For constructs that lacked the GFP tag, GFP was cotransfected. Conventional patch-clamp techniques were used (Kulleperuma et al., 2013) at room temperature (20–26°C). Bath and pipette solutions contained 60–100 mM buffer, 1–2 mM $CaCl_2$ or $MgCl_2$ (intracellular solutions were Ca^{2+} free), 1–2 mM EGTA, and $TMAMeSO_3$ to adjust the osmolality to ∼300 mOsm, titrated with TMAOH. Buffers used were Homo-PIPES (Research Organics) at pH 4.5–5.0, Mes at pH 5.5–6.0, BisTris at pH 6.5, PIPES at pH 7.0, HEPES at pH 7.5, tricine at pH 8.0, CHES at pH 9.0, and CAPS at pH 10.0. Currents are shown without leak correction. To minimize pH_i changes caused by large H^+ fluxes, pulses for large depolarizations in pulse families were sometimes shortened.

The reversal potential (V_{rev}) was determined by two methods, depending on the relative positions of V_{rev} and the threshold voltage for activation of the g_H, $V_{threshold}$. For constructs in which $V_{threshold}$ was positive to V_{rev}, the latter was determined by examining tail currents. Because hH_V1 currents were the only time-dependent conductance present, V_{rev} was established by the amplitude and direction of current decay during deactivation. By using this procedure, time-independent leak or other extraneous conductances do not affect V_{rev} (Morgan and DeCoursey, 2014). Tail currents were not observed in nontransfected cells. For mutants in which $V_{threshold}$ was negative to V_{rev}, it was possible to observe directly the reversal of currents activated during pulse families.

Proton current amplitude (I_H) was usually determined by fitting the rising current with a single exponential and extrapolating to infinite time. Proton conductance (g_H) was calculated from I_H and V_{rev} measured in each solution: $g_H = I_H/(V - V_{rev})$. In some cases where current activation kinetics was difficult to evaluate, g_H was calculated from tail current amplitudes instead of I_H.

To evaluate ΔpH dependence, it is necessary to establish the position of the g_H–V relationship. For this purpose, we have adopted the voltage at which the g_H is 10% of its maximal value as a function of pH ($V_{gH,max/10}$), in preference to other parameters that have been used, such as the midpoint of a Boltzmann distribution or the threshold for activating detectable H^+ current, $V_{threshold}$. Because the g_H–V relationship is steepest at low voltages, fairly large errors in estimating the maximum g_H ($g_{H,max}$) produce only small errors in $V_{gH,max/10}$. This parameter choice avoids the necessity of arbitrarily forcing nonsigmoidal g_H–V data to fit a Boltzmann function (Musset et al., 2008a) or, alternatively, the need to identify the elusive threshold of channel activation, $V_{threshold}$, which is subjective and can be difficult when it occurs near E_H. Nevertheless, $V_{threshold}$ remains useful as a supplemental parameter because its measurement requires minimal current flow and consequently produces negligible pH changes.

Online supplemental material

Fig. S1 shows the sequence of the S4 segment in hH_V1, kH_V1, and EhH_V1, illustrating the conserved Trp in the signature sequence that defines H_V1, RxWRxxR. Fig. S2 shows saturation of the ΔpH dependence of WT kH_V1 (from the dinoflagellate *Karlodinium veneficum*) and of the W176F mutant of kH_V1. Fig. S3 shows the saturation of the ΔpH dependence of WT EhH_V1 (from the coccolithophore *Emiliania huxleyi*) and of W278X mutants of EhH_V1. The online supplemental material is available at http://www.jgp.org/cgi/content/full/jgp.201511456/DC1.

RESULTS

The ΔpH dependence of gating in hH_V1 saturates above pH 8

Perhaps the most remarkable property of H_V1 is the phenomenon of ΔpH-dependent gating. We define ΔpH, the transmembrane pH gradient, as $pH_o - pH_i$. Like other voltage-gated ion channels, H_V1 opens upon depolarization, but the position of the g_H–V relationship is strongly and equally modulated by both pH_o and pH_i, shifting 40 mV for a unit change in either (Cherny et al., 1995). The set point of this relationship is positioned so that the human channel under normal conditions opens only when the electrochemical gradient is outwards. The practical consequence is that channel opening extrudes acid from the cell, which is essential to most of the functions of H_V1.

Fig. 1 illustrates ΔpH-dependent gating of the WT hH_V1. Families of currents recorded in the same cell at four pH_o with pH_i 7 are shown in Fig. 1 (A–D). Channel opening is characteristically slow, especially at lower pH_o. Examination of the corresponding g_H–V (proton conductance–voltage) relationships derived from these currents reveals a −40-mV/U pH shift as pH_o increases (Fig. 1 E). However, the shift between pH_o 8 and pH_o 9 is decidedly less than −40 mV. Saturation of the shift of the g_H–V relationship has not previously been identified in WT H_V1 at either high or low pH_i or pH_o. A <40-mV shift between pH_o 8 and 9 was noted previously and proposed to reflect the approach of pH_o to the pK_a of a site that senses pH_o (Cherny et al., 1995). This interpretation was later questioned when V_{rev} was found to deviate substantially from E_H at extreme pH_o values (pH_o 9–10), and speculatively reinterpreted as reflecting loss of pH_i control at high pH, perhaps because of OH^- transport in rat alveolar epithelial cells (DeCoursey and Cherny, 1997). In the present study, we will show that the attenuation of ΔpH-dependent gating constitutes genuine saturation, because it occurs at a pH where the channel is unequivocally proton selective and pH_i is well established (Fig. 4).

Fig. 1 (G–J) shows WT hH_V1 currents at several pH_i measured in an inside-out patch of membrane, a configuration that allows changing pH_i. Again, activation (channel opening) is slow, increasingly so at high pH_i where the currents become smaller, presumably reflecting the rarity of permeant ions (1 nM H^+ at pH 9). Corresponding g_H–V relationships plotted in Fig. 1 F exhibit a 40-mV/U shift as pH_i increases, but also reveal that the shift appears to saturate between pH_i 8 and pH_i 9. Our

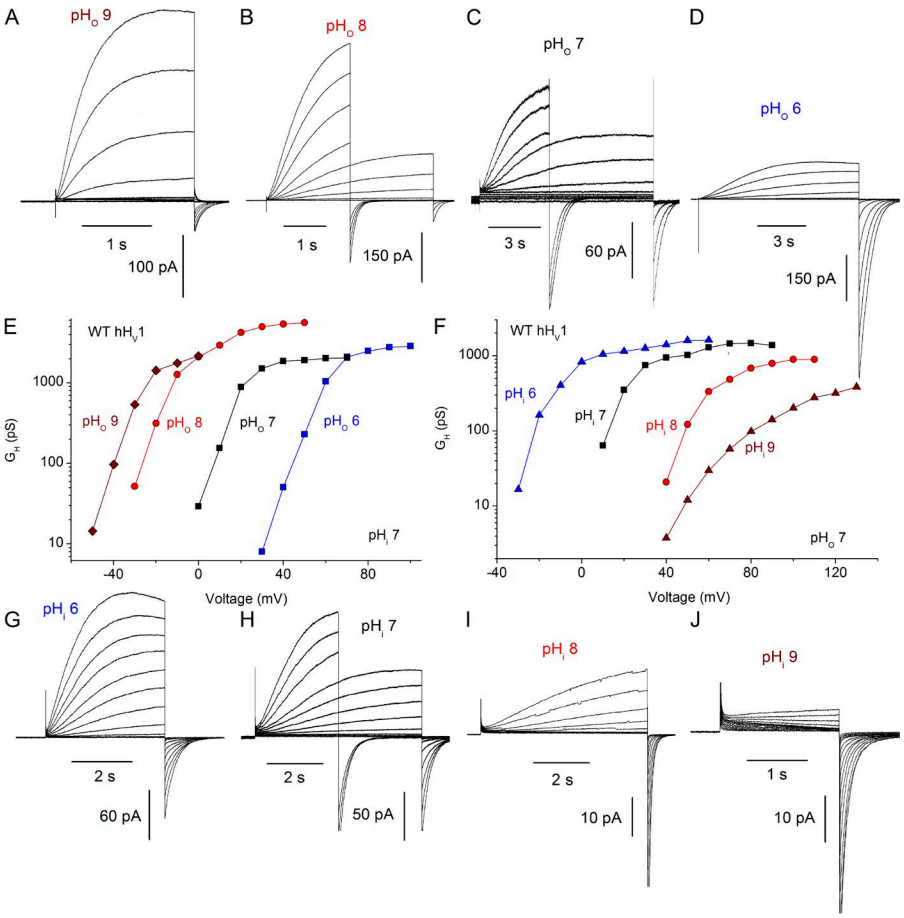

Figure 1. The ΔpH dependence of WT hH_V1 saturates at high pH_o or pH_i. (A–D) Families of currents at several pH_o are illustrated in a COS-7 cell expressing WT hH_V1 with pH_i 7 at holding potentials of −80 (A), −60 (B), or −40 mV (C and D). In some families, shorter pulses were applied for large depolarizations to minimize proton depletion. (E) The g_H–V relationships are plotted, showing that the shift between pH_o 8 and 9 is distinctly <40 mV. Measured V_{rev} in A–D was −95, −53, 5, and 57 mV, respectively. (G–J) Current families in an inside-out patch are shown, with pipette pH_o 7 and holding potentials of −60 (G), −40 mV (H and I), and −20 mV (J), with g_h–V relationships plotted in F. Measured V_{rev} in G–J was −54, 0, 60, and 115 mV, respectively. For g_H calculation, the current amplitude I_H was obtained by fitting rising currents to a single-exponential function, with the exception of J, where because of the difficulty of fitting the slowly activating inward and outward currents, the tail current amplitude was used.

standard procedure is to extrapolate single-exponential fits to obtain "steady-state" current amplitudes. Because the currents in this patch at pH_i 9 were small and activation was exceptionally slow, the g_H was derived from tail currents, which underestimates the g_H. However, $V_{threshold}$ was the same at pH_i 9 as for pH_i 8, indicating a small g_H–V shift. Quantitative values for these shifts are presented later (Figs. 3 and 4). Thus, saturation of ΔpH-dependent gating occurs in WT hH_V1, and it occurs at roughly the same absolute pH whether internal or external pH is varied. The simplest mechanistic explanation is that ΔpH dependence is caused by titration of a site with pK_a of >8 that is accessible from either side of the membrane. In the first (and only) model proposed to explain ΔpH-dependent gating (Cherny et al., 1995), the same group(s) sensed pH_i and pH_o but was (were) required to be accessible only to one side of the membrane at a time. The data on WT hH_V1 up to this point are consistent with this idea, which invokes a single pH-sensing site that has alternating access.

Mutations to Trp^{207} in hH_V1 compromise ΔpH-dependent gating

We replaced the bulky Trp^{207} in the human proton channel, hH_V1, with Ala, Phe, or Ser, designating the mutants W207A, W207F, and W207S, respectively. All mutants generated similar voltage- and time-dependent currents. Because we could not distinguish among the properties of these three mutants, their data are combined in data summaries and termed "W207X." Families of currents recorded in the W207A mutant at four pH_o in Fig. 2 (A–D) reveal several noteworthy differences from WT hH_V1. Most prominently, channel opening was two orders of magnitude faster, as will be described below (Fig. 5). Also evident is that the absolute position of the g_H–V relationship tended to be more negative, resulting in pronounced inward currents at lower pH_o (Fig. 2, C and D), also evident in the current–voltage relationships (Fig. 2 E). The voltage at which the g_H was 10% of its maximal value, $g_{H,max}$, in whole-cells and inside-out patches at symmetrical pH 7.0 was variable but averaged 9.8 ± 2.6 mV (mean ± SEM; n = 14) in

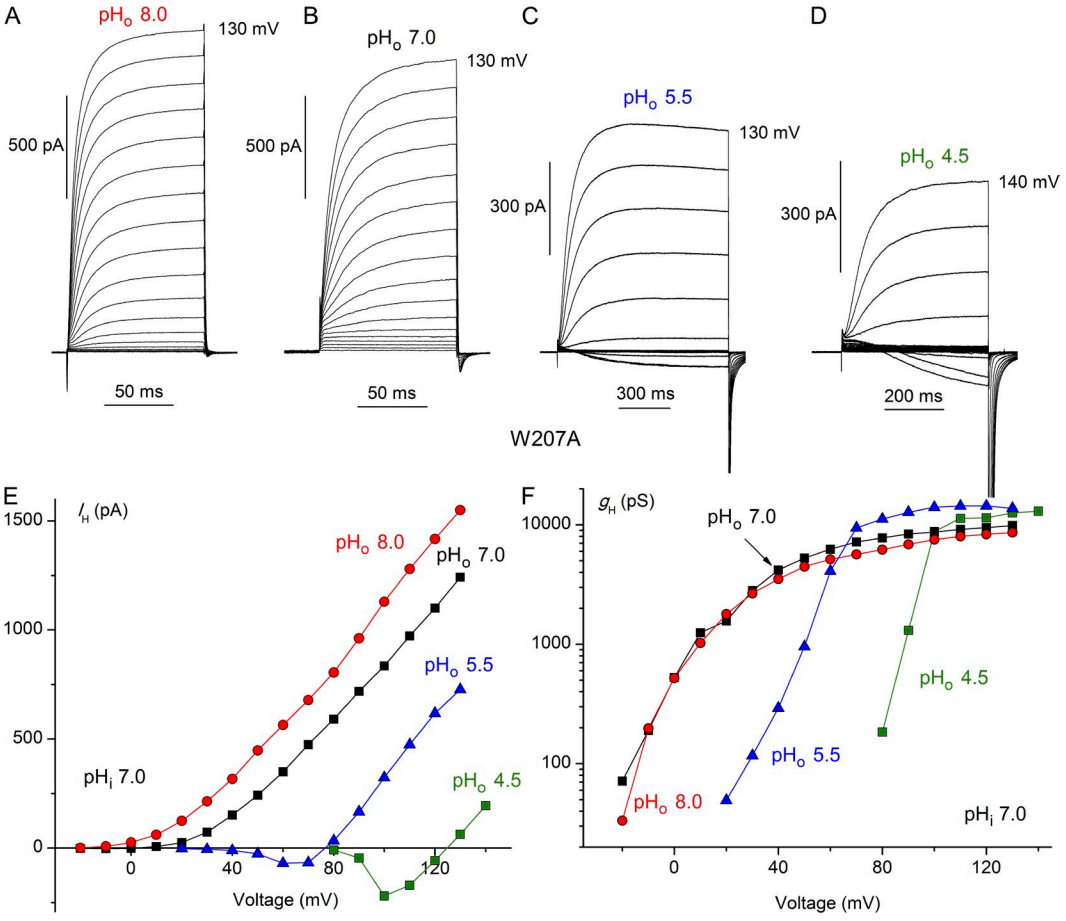

Figure 2. Modified pH_o sensitivity of W207A mutant hH_V1. Families of proton currents at several pH_o in a cell with pH_i 7.0 are illustrated (A–D). Pulses were applied in 10-mV increments up to the voltage indicated, from a holding potential of −60 (A) or −40 mV (B–D). (E) Proton current amplitudes (I_H) from the cell in A–D were obtained by fitting the rising current with a single exponential and extrapolating to infinite time. (F) Proton conductance (g_H) was calculated from the currents in E using V_{rev} measured in each solution.

WT hH_V1 and −8.1 ± 3.3 mV (n = 20) in W207X mutants ($P < 0.001$).

More subtly, although voltage-dependent gating was shifted negatively by increases in pH_o (Fig. 2, E and F), as in all known H_V1, closer inspection reveals that the hallmark ΔpH dependence is altered in Trp^{207} mutants. When pH_o was increased from 4.5 to 5.5 to 7.0, the ubiquitous 40-mV/U shift in the g_H–V relationship (Cherny et al., 1995; DeCoursey, 2003) occurred (Fig. 2 F). However, above pH_o 7.0, there was no further shift; thus, saturation of the shift occurred at ~1.5 U lower pH_o than in WT (Fig. 1 E). If the mechanism by which ΔpH-dependent gating occurs involves one or more titratable groups, as has been proposed (Cherny et al., 1995), then replacement of Trp^{207} apparently lowers the effective pK_a of this group(s).

To provide a more concise and quantitative way to evaluate ΔpH dependence, in Fig. 3 we plot the voltage at which the g_H is 10% of its maximal value ($V_{gH,max/10}$) as a function of pH (discussed in Materials and methods). Fig. 3 (A and B) reiterates the observation from Fig. 1 that pH_o and pH_i dependence of gating both change with a slope of 40 mV/U (dashed reference lines in all figures) over a wide range of pH, and both saturate between pH 8 and 9 in WT hH_V1. An important additional result is that Fig. 3 (A and B) indicates that the saturation with pH_o or pH_i occurs independently of pH_i or pH_o, respectively. Thus, for example, in Fig. 3 B saturation occurred similarly above pH_i 8 at either pH_o 7 or 8. Evidently, saturation occurs at a particular absolute pH_o or pH_i, rather than at a particular ΔpH. This result is consistent with the titration of one or more specific protonation sites that sense pH on only one side of the membrane. Hence, this result contradicts the simplest mechanism of a single site with alternating access to both sides of the membrane.

Analogous plots for the Trp^{207} mutants (Fig. 3 C) show that their pH_o dependence is fully saturated at pH_o ≥7.0, at least 1 U lower than in WT, with no further shift of the g_H–V relationship up to pH_o 10, confirming the impression from Fig. 2. Notably, the pH_i dependence did not saturate up to pH_i 8 (Fig. 3 D), and thus in contrast to WT, the saturating pH differs for pH_o and pH_i in the Trp^{207} mutants. This result also speaks

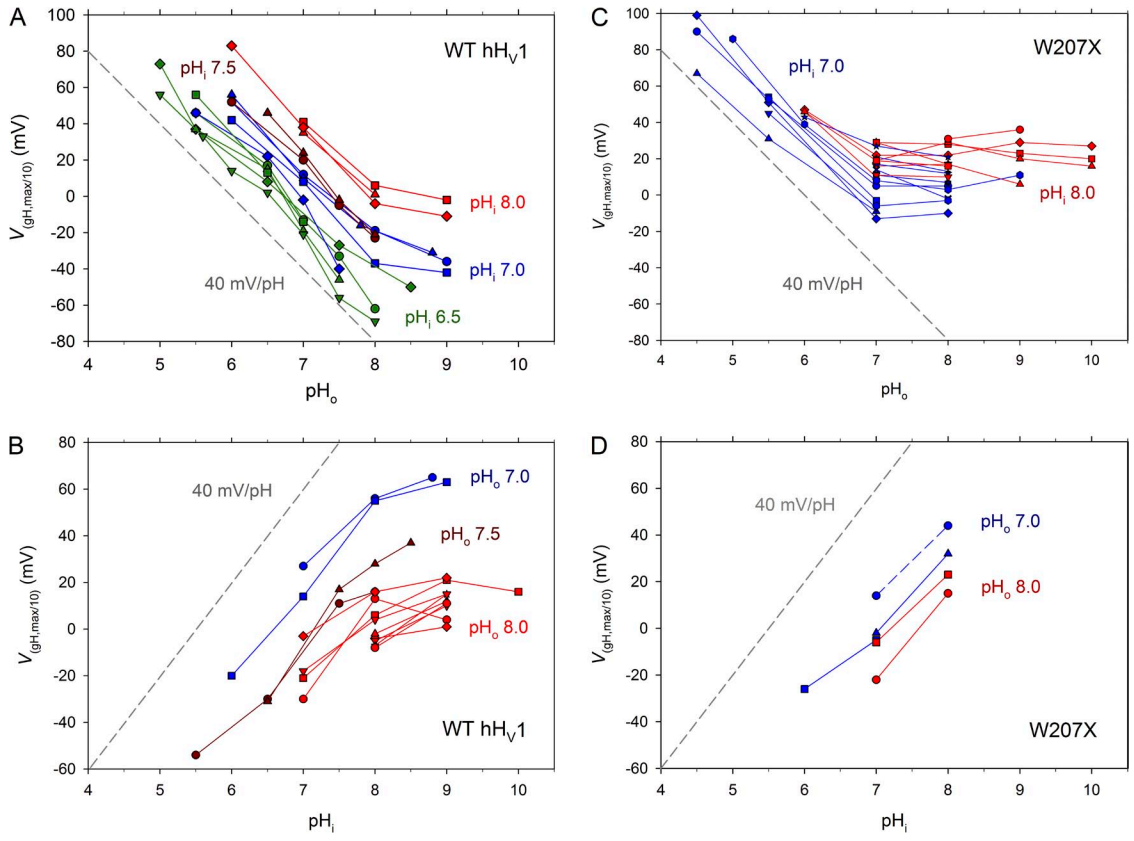

Figure 3. Saturation of the ΔpH dependence of WT hH_V1 (A and B) and of W207X mutants of hH_V1 (C and D). The voltage at which g_H is 10% maximal ($V_{gH,max/10}$) is plotted as a function of pH_o (A and C) or pH_i (B and D), with lines connecting measurements in the same cell. In whole-cell measurements, pH_i is color coded, as indicated. In inside-out patches, pH_o is color coded, as indicated. For reference, the dashed gray line in each graph shows the slope of the ubiquitous 40-mV/U ΔpH shift in the g_H–V relationship (Cherny et al., 1995; DeCoursey, 2003); the horizontal position of this line is arbitrary. (C) Data from 13 W207A, eight W207F, and two W207S cells. (D) Data from three W207A, one W207F, and one W207S patch. No differences were detected among the Trp replacements.

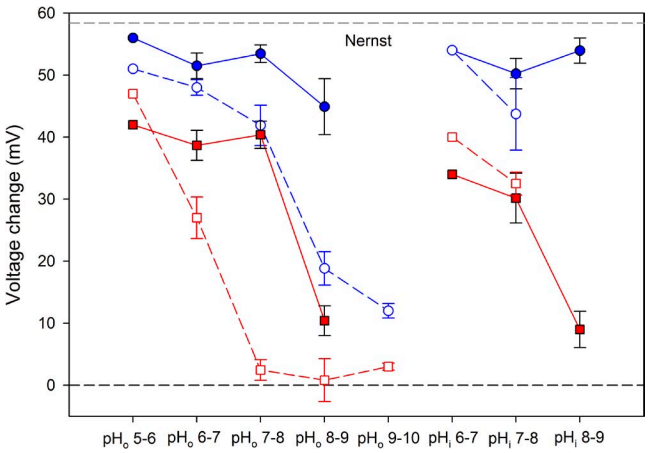

Figure 4. Saturation of ΔpH-dependent gating occurs independently of loss of proton selectivity of Trp^{207} mutants. The mean ± SEM (error bars) change in V_{rev} for a 1-U change in pH is plotted for WT hH$_V$1 (closed blue circles) and for W207X (open blue circles). The shift in $V_{gH,max/10}$ in the same cells is also plotted for WT hH$_V$1 (closed red squares) and for W207X (open red squares). Numbers of cells for both parameters are one, six, eight, and five for increasing pH$_o$ in WT; one, six, and eight for increasing pH$_i$ in WT; one, five, 11, six, and three for increasing pH$_o$ in W207X; and one and four for increasing pH$_i$ in W207X. The difference in V_{rev} in W207X versus WT was significant at pH$_o$ 7–8 ($P < 0.02$) and 8–9 ($P < 0.001$). The difference in $V_{gH,max/10}$ in W207X versus WT was significant at pH$_o$ 6–7 ($P < 0.02$) and 7–8 ($P < 0.0001$).

against the idea that the same group might sense pH on both sides of the membrane (with alternating access), because in the Trp^{207} mutants, the pK_a of the site(s) that sense pH$_o$ and pH$_i$ differ. An alternative interpretation that cannot be formally ruled out is that moving a single group to a different local environment might itself alter its pK_a. In any event, the presence or absence of Trp^{207} evidently modulates either the accessibility of the pH-sensing site to the external solution or the effective pK_a of the site(s), or both.

A different analysis of the data is shown in Fig. 4. Solid red squares show that the change in $V_{gH,max/10}$ for a 1-U change in pH$_o$ or pH$_i$ in WT is roughly 40 mV, but it drops precipitously to ∼10 mV at pH$_o$ or pH$_i$ 8–9. For W207X (open red squares), the shift is already depressed at pH$_o$ 6–7 and is abolished (drops to ∼0 mV) at higher pH$_o$ (7–8, 8–9, and 9–10). In contrast, the W207X mutants exhibit no loss of ΔpH dependence up to pH$_i$ 7–8, emphasizing that the W207X mutation appears to selectively alter pH$_o$ but not pH$_i$ sensing. This result supports the idea of distinct external and internal pH sensors.

Mutations to Trp^{207} in hH$_V$1 facilitate channel opening

Another distinctive consequence of replacing Trp^{207} was faster channel opening, evident in Fig. 2. The turn-on of current during depolarizing pulses reflects the time course of channels opening. The rising currents were fitted with a single exponential to obtain τ_{act}, the time constant of activation (channel opening). Mean τ_{act} values plotted in Fig. 5 show that channel opening was ∼100 times faster than WT for each of the Trp^{207} mutants. WT kinetics was more variable than that of any of the mutants, perhaps reflecting the stronger temperature sensitivity of WT H$_V$1 (DeCoursey and Cherny, 1998; Kuno et al., 2009) or variable proton depletion during the much longer pulses required to determine

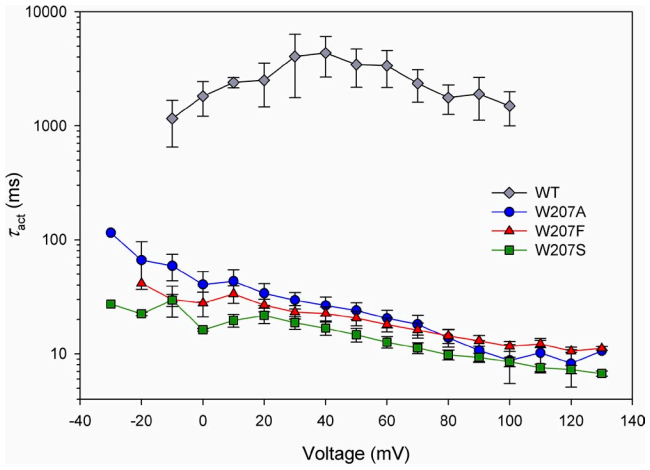

Figure 5. Replacement of Trp^{207} greatly accelerates hH$_V$1 opening. The activation time constant, τ_{act}, was obtained by fitting rising currents to a single exponential. All measurements were done at symmetrical pH 7.0 but include both whole-cell and excised inside-out patch data. Error bars represent mean ± SEM, with n = 7, 9, and 8 for W207F, W207S, and W207A, respectively; WT includes five cells and seven inside-out patches.

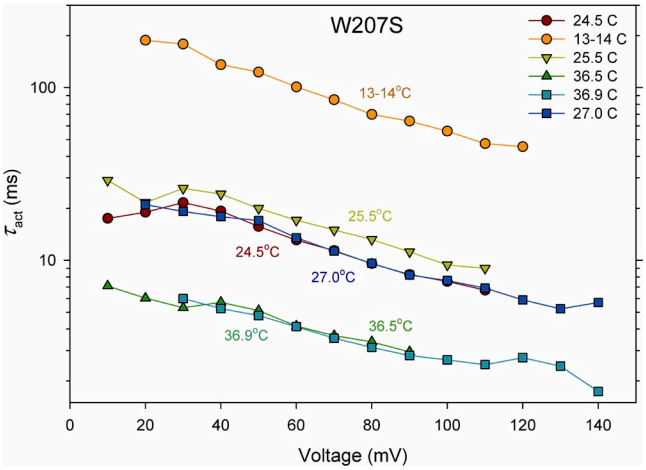

Figure 6. Replacement of Trp^{207} decreases the Arrhenius activation energy for hH$_V$1 opening. The activation time constant, τ_{act}, was determined in one cell during families of pulses at various temperatures at symmetrical pH 7. The sequence is indicated in the inset. The Q_{10} was somewhat higher at lower voltages (e.g., 4.3 at 20 mV and 3.7 at 100 mV, for the entire temperature range). As reported previously for native H$_V$1 (DeCoursey and Cherny, 1998), E_a also increased at lower temperatures. Temperature drift during families of pulses was on the order of 1°C.

WT kinetics. Surprisingly, replacement of Trp with an aliphatic hydrophobic residue (Ala), a polar hydrophilic residue (Ser), or an aromatic residue (Phe) produced identically profound acceleration of activation. The kinetic consequences of Trp at position 207 appear to be unique and unrelated to such generic qualities as hydrophobicity, polarity, or aromaticity.

Channel-closing kinetics was examined by measuring τ_{tail}, the time constant of tail current decay (deactivation). Measured at symmetrical pH 7.0 at −40 mV, τ_{tail} was 227 ± 22 ms (n = 16) in WT hH_V1 and 29 times faster in the three Trp^{207} mutants (7.8 ± 0.8 ms; n = 17).

If the slowing of gating by Trp^{207} were rate determining in WT channels, then the activation energy, E_a for gating should be lower in mutants than the 30–38 kcal/mol in WT channels (DeCoursey and Cherny, 1998). Fig. 6 illustrates that this was the case. The time constant of channel opening (τ_{act}) was determined by fitting rising currents with a single-exponential function in current families recorded at several temperatures. The Arrhenius activation energy, E_a, was calculated from $E_a = RT_1T_2/(T_2 - T_1)\ \ln(\tau_{act,1}/\tau_{act,2})$, where R is the gas constant (1.9872 cal K^{-1} mol^{-1}) and T_1 and T_2 are the lower and higher temperatures (in K) (DeCoursey and Cherny, 1998). In three experiments (two whole cell and one inside-out patch), E_a determined over the entire temperature range from 11–13 to 35–37°C averaged ~22 kcal/mol. Therefore, the process involved in slow WT activation that is regulated by Trp^{207} is rate limiting.

Mutations to Trp^{207} in hH_V1 compromise proton selectivity

Central to performing all of the functions of H_V1 is its perfect proton selectivity. Proton selectivity was evaluated by measuring the reversal potential, V_{rev}, at various pH. Because replacing Trp^{207} shifted the g_H–V relationship negatively, at some ΔpH, V_{rev} could be observed directly as reversal of the current during families of pulses, as illustrated in Fig. 7 (A and C). Alternatively, V_{rev} can be estimated in the usual manner using tail currents (Fig. 7, E and F). Surprisingly, there was only a small shift in V_{rev} (<20 mV) between pH_o 8 and 9 in the W207F mutant (Fig. 7, E and F). In comparison, the same pH_o change produced a nearly Nernstian (58-mV) shift in the WT hH_V1 (Fig. 7, G and H). The replacement of Trp^{207} compromised proton selectivity.

Fig. 8 A confirms the proton specificity of the WT hH_V1. The reversal potential, V_{rev}, measured over a wide range of pH_o (5.0–9.0) and pH_i (5.5–9.0) was close to

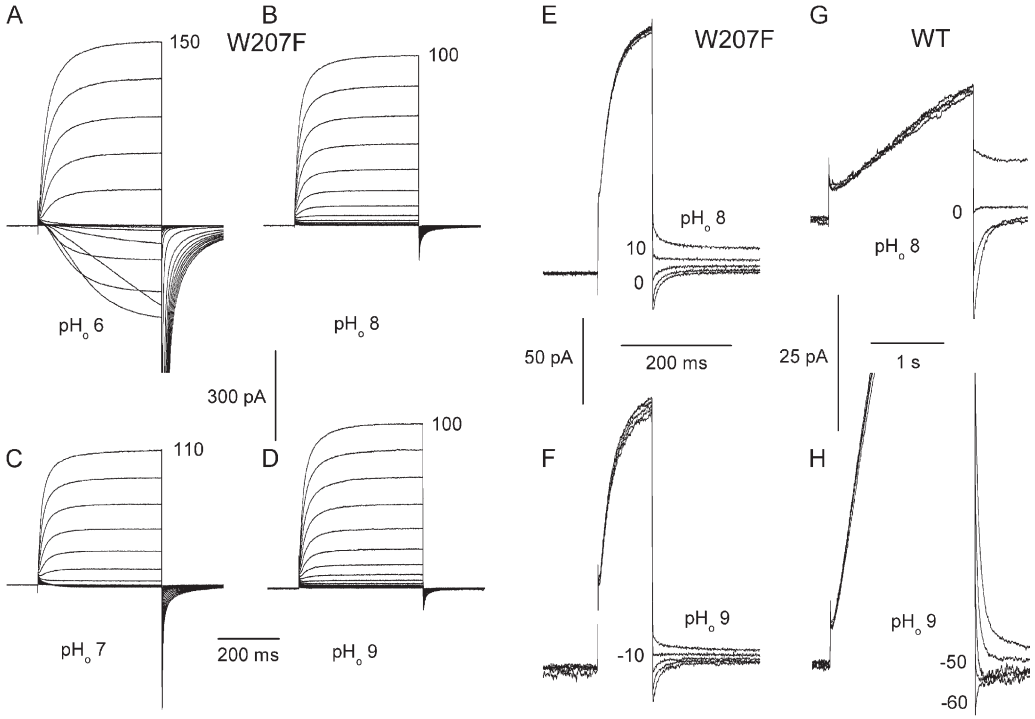

Figure 7. Measurement of V_{rev} in W207F and in WT hH_V1. (A–D) Families of currents in a cell expressing W207F channels were elicited by depolarizing pulses applied in 10-mV increments up to the voltage shown. When it is positive to $V_{threshold}$, V_{rev} is easily obtained by interpolating between inward and outward currents, as in families at pH_o 6 (A) or 7 (C). In the same cell at pH_o 8 (B and E) and 9 (D and F), V_{rev} was extracted from the reversal of tail currents. In this cell, V_{rev} at pH_o 6, 7, 8, and 9 was 102, 52, 7, and −10 mV; E_H was 117, 58, 0, and −58 mV, respectively. Loss of proton selectivity is indicated by the large deviation of V_{rev} from E_H at high pH_o. In WT hH_V1, the shift in V_{rev} obtained by tail currents at pH_o 8 (G) and 9 (H) was nearly Nernstian. Both cells in this figure contained pH_i 8 solutions. The holding potential was −20 (G), −30 (C), −40 (A, B, E, and H), or −60 mV (D and F). Prepulses were to 60 (E and F), 20 (G), or 10 mV (H).

the Nernst potential, E_H, shown as a dashed line. Surprisingly, Trp^{207} mutants were imperfectly proton selective. Fig. 8 B shows that although they were highly selective at neutral and acidic pH, at high pH_o (8–10), the measured reversal potential, V_{rev}, deviated consistently and substantially from E_H.

The mean shift in V_{rev} for a 1-U change in pH is plotted in Fig. 4 (blue circles). The V_{rev} of WT hH_V1 (closed blue circles) was reasonably near E_H at all pH studied, whereas V_{rev} of the W207X mutants (open blue circles) was distinctly sub-Nernstian at pH_o 8–10, being significantly lower than WT at pH_o 7–8 and 8–9. Trp^{207} mutation produces loss of proton selectivity, but only at high pH_o.

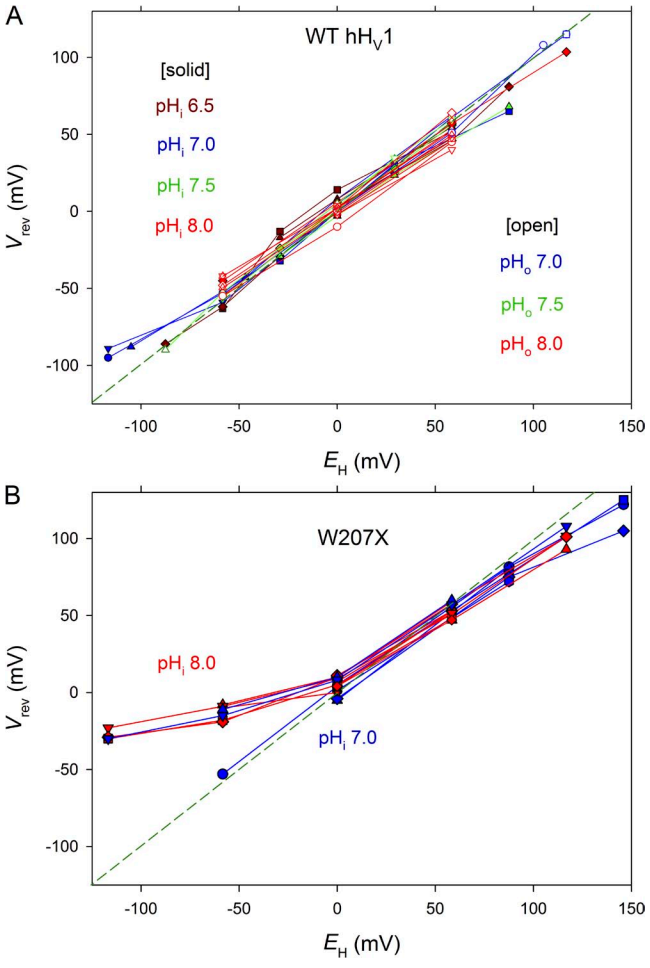

Figure 8. Proton selectivity is perfect in WT hH_V1 (A) but compromised in Trp^{207} mutants (B). Proton selectivity is indicated by the proximity of measured values of V_{rev} and the Nernst potential for H^+, E_H. Data were obtained in whole-cell (closed symbols) and inside-out patch configuration (open symbols). In whole-cell measurements, the color-coded pH_i solution was in the pipette, and pH_o was varied, with lines connecting measurements in each cell. In inside-out patch measurements, pH_o was the pipette solution and pH_i was varied. Whole-cell measurements in B include eight W207F, 12 W207A, and one W207S cell. For W207X mutants, currents in patches were too small to allow reliable estimation of V_{rev}.

Replacement of Trp in a dinoflagellate H_V1 (kH_V1) speeds activation

Given that replacing Trp greatly speeds activation in hH_V1, we were curious as to whether the same would be true in other species. To make this test rigorous, we selected an evolutionarily distant species in which the amino acid identity with hH_V1 is only 15%, namely *K. veneficum* (Smith et al., 2011). We made the same three substitutions to the corresponding Trp^{176} in kH_V1 (Fig. S1): W176A, W176F, and W176S. These mutants generated proton-selective currents in the pH range explored that exhibited qualitatively similar changes when pH_o was changed (Fig. 9, A vs. B, and C vs. D). Like their human counterparts, the Trp mutants activated extremely rapidly. Activation time constants were nearly two orders of magnitude faster than in the WT channel (Fig. 9 E). WT closing kinetics was faster in kH_V1 than in hH_V1, and in the Trp^{176} mutants, tail current decay was often too fast to distinguish reliably from capacity transients. Mirroring the pattern seen in the human Trp mutants, τ_{act} was roughly the same whether Trp^{176} was replaced by Ser, Ala, or Phe (Fig. 9 E). The same remarkable result obtained in both species is that Trp in the signature sequence (RxWRxxR) profoundly slows channel opening by a mechanism that other amino acids tested are unable to replicate. This result suggests a quite specific type of interaction.

The kH_V1 channel does exhibit ΔpH-dependent gating, although its absolute voltage range of opening is 60 mV more negative than in other species (Smith et al., 2011). Therefore, it was of interest to determine whether saturation of this effect occurs. In WT kH_V1, saturation was observed above pH_o 8.0 or pH_i 8.0 (Fig. S2), similar to the pH at which saturation occurs in WT hH_V1. Also like hH_V1, Trp mutation compromised ΔpH dependence, with saturation occurring at lower pH_o in the W176F mutant (Fig. S2 C).

Replacement of Trp in a coccolithophore H_V1 (EhH_V1) speeds activation and shifts the g_H–V relationship negatively

To further test the generality of the roles of Trp, we produced analogous mutations in the coccolithophore, *E. huxleyi* H_V1 (EhH_V1), namely W278A, W278S, and W278F (Fig. S1). The EhH_V1 sequence differs drastically from hH_V1, with only 18% identity, as well as from kH_V1, with 29% identity. Fig. 10 shows that activation kinetics was also faster in the EhH_V1 when Trp^{278} was replaced, although the effect was smaller than in the other species examined. Opening of these mutants was accelerated four- to sixfold in the positive voltage range.

Another pronounced change in EhH_V1 mutants was a negative shift of the g_H–V relationship, with the voltage at which the g_H was 10% of $g_{H,max}$ averaging −5.2 ± 2.9 (12) in WT EhH_V1 and −33.4 ± 2.3 (14) in the mutants, a −28-mV shift. Some of the slowing of τ_{act} may be

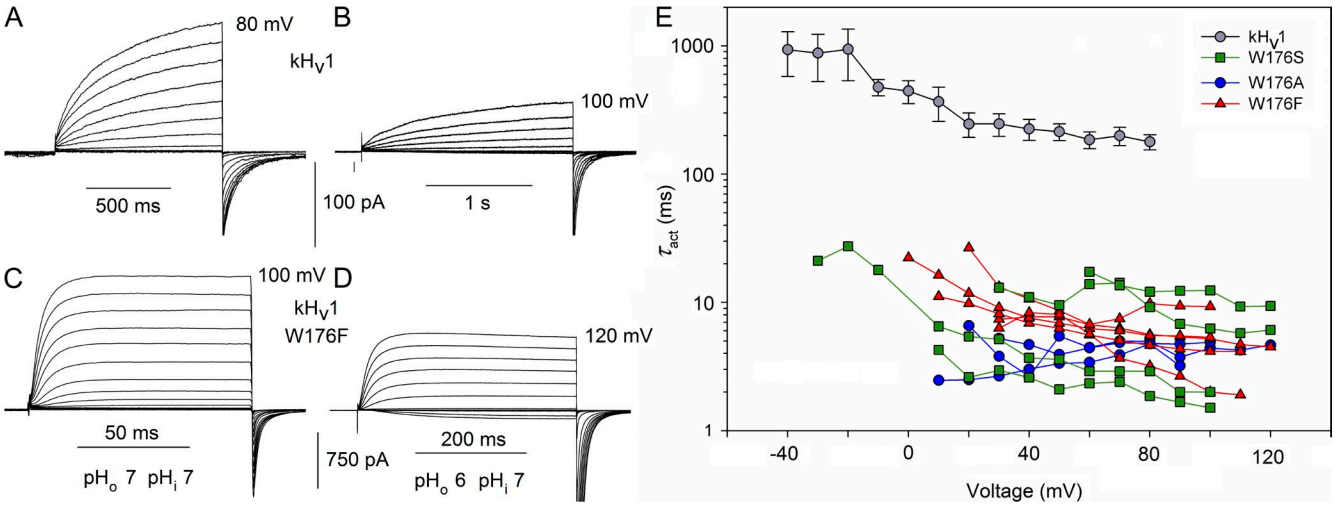

Figure 9. The W176F mutation in the dinoflagellate kH_V1 accelerates channel opening. Families of currents in WT kHv1 (A and B) and in the W176F mutant (C and D), studied at pH_o 7 (A and C) or 6 (B and D), as indicated, all at pH_i 7. Note the different time scales. Voltage steps were applied in 10-mV increments to the final voltage indicated. The holding potential was −60 (A and C) or −40 mV (B and D). (E) Replacement of Trp^{176} in the dinoflagellate kH_V1 with Ala, Ser, or Phe hastens channel opening to the same extent. The activation time constant, τ_{act}, was determined by fitting the turn-on of current with a single rising exponential. The WT channel kinetics (mean ± SEM; n = 5–14) was extracted from data for a previous study, all at symmetrical pH 7.0 (Smith et al., 2011). Single mutants, as indicated, were expressed in HEK-293 or COS-7 cells. Measurements were performed in whole-cell configuration at symmetrical pH 7. Data from each cell are connected by lines.

ascribable to this shift; the peak value of τ_{act} occurs in a more negative voltage range in W278X than in WT.

Intriguingly, the ΔpH dependence of EhH_V1 appeared consistently steeper (∼50 mV/U pH) both for changes in pH_o and pH_i than in H_V1 in other species (Fig. S3). Saturation of ΔpH dependence was evident only above

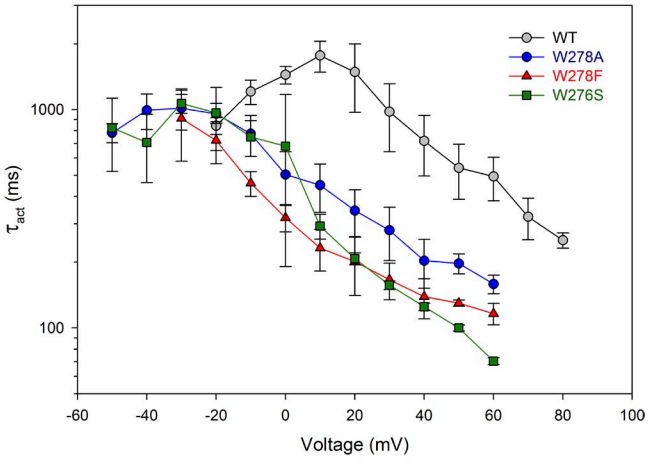

Figure 10. Replacement of Trp^{278} in the coccolithophore EhH_V1 with Ala, Ser, or Phe hastens channel opening to the same extent. The activation time constant, τ_{act}, was determined by fitting the turn-on of current with a single rising exponential. The mean ratio of WT/W278X within the range of 10–60 mV was 3.5 (W278A), 5.7 (W278F), and 6.3 (W278S). Numbers of cells are: WT, three to six; W278A, three to four; W278F; two to four; W278S, two to three. Single mutants were expressed in HEK-293 or COS-7 cells, and measurements were performed in whole-cell configuration at symmetrical pH 7. Error bars represent mean ± SEM.

pH_o 8.0 in WT, essentially identical to both hH_V1 and kH_V1. No significant change in this property was detected in the EhH_V1 mutants, although the mean shift from pH_o 7 to pH_o 8 decreased from −53 ± 2 mV (SEM; n = 4) in WT to −43 ± 5 mV (n = 4) in mutants. The ΔpH dependence of EhH_V1 would thus be maintained reasonably well over the normal pH range experienced by coccolithophores; the pH of seawater is 7.5–8.4 (Chester and Jickells, 2012). That saturation of ΔpH-dependent gating occurred at the same pH_o and pH_i in all three species suggests that the same or similar group(s) may be involved in pH sensing.

DISCUSSION

Activation kinetics

Cation–π interaction between Trp^{207} and Arg^{211} in hH_V1 latches the channel closed. The most obvious effect of replacing Trp^{207} with smaller amino acids was acceleration of channel opening by two orders of magnitude. The precise physical mechanism by which Trp slows WT H_V1 opening can only be speculated, but several possibilities exist. In the closed mH_V1 structure (78% sequence identity to hH_V1), Trp is oriented toward the lipid (Takeshita et al., 2014), suggesting that hydrophobic interactions might stabilize it in this position. Hydrophobic interactions with membrane lipids have been considered for closed-state stabilization by Val^{363} in the *Shaker* K^+ channel VSD (Lacroix et al., 2013). However, the aromatic Phe, which engages in purely hydrophobic interactions (Killian and von Heijne, 2000),

does not share this behavior in H_V1. In all three species studied here, the Trp→Phe mutant did not exhibit intermediate behavior but rather activated as rapidly as Trp→Ser or Trp→Ala mutants. This result suggests that the ambivalence of Trp in having a polar amide group plays a key role. As discussed in the Introduction, the mH_V1 structure (Takeshita et al., 2014) appears to indicate that Trp engages in cation–π interaction with R3, stabilizing the closed structure. In fact, Trp^{207} and Arg^{211} are an example of the second most common cation–π interaction that occurs within α helices between residues *i* and (*i* + 4) (Gallivan and Dougherty, 1999).

The portion of mH_V1 containing Trp and R3 is compared with the corresponding region in the *Ciona intestinalis* voltage-sensing phosphatase (CiVSP) in Fig. 11, with both proteins considered to be in their closed or "down" position. It seems surprising that in both structures, R3 appears to lack direct aqueous contact. Burying acidic or basic amino acids can shift their pK_a by as much as 5 pH units, but Arg is the most likely to remain ionized (Kim et al., 2005). In fact, Arg appears uniquely able to remain protonated inside proteins (Harms et al., 2011). In the down structure of CiVSP, R3 is found in a pocket surrounded by hydrophobic residues that faces away from the center of the VSD; the guanidinium group of R3 is oriented somewhat "sideways" to the plane of the lipid and it salt-bridges with Asp^{186} (Fig. 11 A). In the mH_V1 structure (Fig. 11 B), Trp^{203} appears to provide part of a similar pocket in which R3 interacts both with Asp^{170} (equivalent to Asp^{174} in hHv1 and Asp^{186} in CiVSP) and with Asn^{210}, although in this structure the guanidinium of R3 appears to be pointing nearly directly away from the center of the channel (Fig. 11 B). We speculate that Phe may be unable to stabilize R3 in this position, possibly because of Phe's weaker cation–π interaction capability. The electrostatic R3–Asp interaction in closed H_V1 may also contribute a stabilizing function like that of the corresponding Lys^{374}–Asp^{316} in the closed *Shaker* K^+ channel VSD (Papazian et al., 1995). In all open H_V1 models (Ramsey et al., 2010; Wood et al., 2012; Kulleperuma et al., 2013; Chamberlin et al., 2014), R3 has rotated to face the pore, whereas Trp still appears to face the lipid. For this kind of conformational change to occur during opening, the interactions between the Trp–Arg pair would have to be disrupted. The much more rapid opening in the W207X mutants may reflect the absence of these stabilizing interactions.

The faster activation kinetics after Trp mutation in hH_V1 qualitatively resembles that seen in forced monomerization. Monomeric constructs open four to seven times faster than their dimeric counterparts (Koch et al., 2008; Tombola et al., 2008; Musset et al., 2010; Fujiwara et al., 2012). Might Trp mutation eliminate interaction at the dimer interface between Trps from each protomer that normally contribute to closed-state stabilization? This notion is contradicted by a cysteine cross-linking study indicating that the two S4 helices appear not to interact (Lee et al., 2008). On the other hand, the S4 segments are close to each other in a proposed dimer model based on the closed structure of mH_V1 (Takeshita et al., 2014).

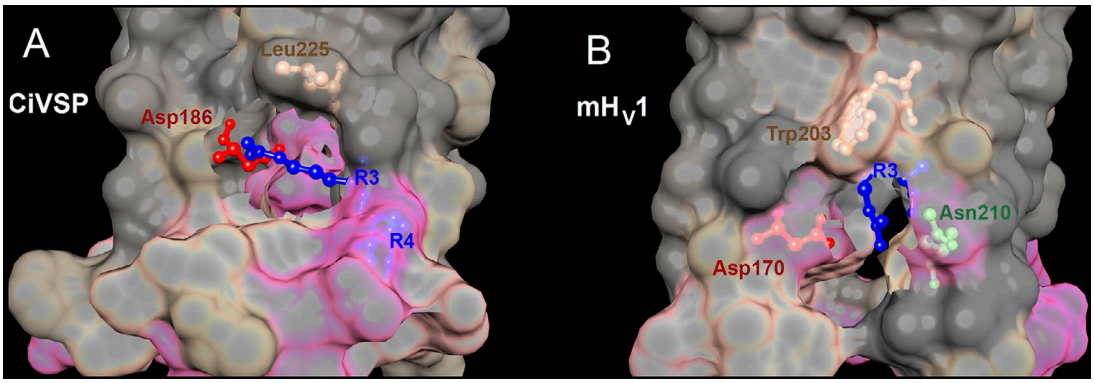

Figure 11. Crystal structures of CiVSP in the "down" state and mH_V1 chimera in the closed state reveal pockets that enclose electrostatic interactions involving R3. The crystal structures of the down state of CiVSP (A) (Li et al., 2014) and the closed mH_V1 chimera (B) (Takeshita et al., 2014) were superimposed with the same orientation. The top is toward the extracellular surface, and the view is from the side. The interfacial surface between protein and lipid is cut away to show the pocket containing R3 and its interacting partners. Local hydrophobicity is indicated by gray (hydrophobic), tan (intermediate), and pink (hydrophilic). (A) In the down structure of CiVSP (Protein Data Bank [PDB] accession no. 4G80), which is more closely related to H_V1 phylogenetically than is the VSD of other ion channels (Smith et al., 2011), R3 faces away from the center of the VSD. The guanidinium group of R3 forms a salt-bridge with Asp^{186}. (B) In the closed structure of mH_V1 (PDB accession no. 3WKV), Trp^{203} and R3 both face away from the center of the channel; the guanidinium of R3 appears to point nearly directly away from the center of the channel. In the mH_V1 structure, Trp^{203} forms the roof of the pocket, in which R3 interacts both with Asp^{170} (equivalent to Asp^{174} in hH_V1 and Asp^{186} in CiVSP) and with Asn^{210}. Molecular graphics and analyses were performed with the University of California, San Francisco (UCSF), Chimera package (resource for Biocomputing, Visualization, and Informatics, UCSF, San Francisco; supported by NIGMS P41-GM103311) (Pettersen et al., 2004).

Is it possible that the primary reason for the conservation of Trp^{207} is to slow gating? It is not immediately obvious why slow H_V1 activation would be evolutionarily advantageous. On the other hand, rapid opening would not confer any advantage for most of the functions proposed for H_V1 in mammalian cells. For example, H_V1 is activated in phagocytes to compensate for the electrogenic activity NADPH oxidase (Henderson et al., 1987; DeCoursey et al., 2003); the latter enzyme is turned on by most stimuli only after a delay and on a time scale of seconds (DeCoursey and Ligeti, 2005). In cells in which acid extrusion via H_V1 occurs for the purpose of pH homeostasis or signaling, such as airway epithelia (Fischer, 2012), basophils (Musset et al., 2008b), B lymphocytes (Capasso et al., 2010), neutrophils (Morgan et al., 2009), or sperm (Lishko et al., 2010), rapid opening is less important than simply remaining open as long as necessary. The absence of inactivation is thus arguably more critical than rapid activation would be. Another possibility is that because a single *HVCN1* gene codes for proton channels in a multiplicity of cell types in which H_V1 serves diverse purposes, the properties of the protein must be compatible with the physiology of all cells. An excitable cell might be ill-served by a rapidly activating proton channel that could interfere with the action potential.

Trp^{207} in hH_V1 anchors the S4 segment and stabilizes the closed channel. By retarding channel opening by 100-fold, while slowing closing only 29-fold, Trp^{207} might tend to produce a net stabilization of the closed state. In fact, Trp^{207} mutants did activate at voltages 18 mV more negative than WT hH_V1; therefore Trp^{207} does contribute to stabilizing a closed state. Native proton channels open almost exclusively positive to E_H and thus never produce significant inward current (DeCoursey, 2003). The negative shift of the g_H–V relationship in Trp^{207} mutants resulted in distinct inward currents just above $V_{threshold}$, especially with inward H^+ gradients (e.g., Figs. 2, C–E, and 7, A and C). Substitution of Trp^{207} thus subverts this principal feature of H_V1 and compromises the task of proton extrusion. One could speculate that Trp^{207} fine tunes the voltage dependence of H_V1 to prevent premature opening. Because of the proximity of $V_{threshold}$ and V_{rev} in WT H_V1 (Cherny et al., 1995; Musset et al., 2008a), without the stabilization of the closed state by Trp^{207}, channel opening would result in proton influx. Given that mammalian cells are largely concerned with extrusion of metabolically produced acid (Roos and Boron, 1981), such a propensity would be deleterious to cell homeostasis.

In EhH_V1, Trp also decidedly stabilized the closed state; the g_H–V relationship was 28 mV more negative in W278X mutants than in WT. In contrast, W176X mutants in kH_V1 activated 25 mV more positively than WT. The atypical behavior of kH_V1 in this regard may reflect distinct teleological considerations. EhH_V1 exists to extrude acid (Taylor et al., 2011), and like hH_V1, must therefore be poised to open just above E_H. In contrast, kH_V1 activates 60 mV more negatively than H_V1 in any other species (Smith et al., 2011), which is ideal for its quite different function in dinoflagellates of mediating H^+ influx that triggers the flash in bioluminescent species (Fogel and Hastings, 1972). The molecular mechanism responsible for the unique kH_V1 voltage dependence is unknown.

Temperature dependence

The gating kinetics of H_V1 in several mammalian cells is extraordinarily temperature dependent, with Q_{10} values of 6–9 (E_a for the delay, τ_{act}, and τ_{tail} were identically 30–38 kcal/mol) (DeCoursey and Cherny, 1998). The Arrhenius activation energy, E_a, of channel opening (τ_{act}) of W207S was 20–25 kcal/mol (Q_{10} of 3.5–4.0), distinctly smaller than in WT, indicating that the factors that establish the kinetics in W-free H_V1 have more modest E_a. Evidently, the perfectly conserved Trp^{207} is the dominant contributor to the exotic temperature sensitivity of WT hH_V1, and replacing it lowers the Q_{10} of gating into the range of most ordinary ion channels; two dozen examples are given in Table II of DeCoursey and Cherny (1998). That Trp is involved in the rate-limiting step in H_V1 opening is consistent with the idea that opening a closed H_V1 requires disrupting the cation–π interactions between Trp and Arg, and perhaps also inter-protomer Trp–Trp interactions in the dimer that stabilize closed channels.

The gating kinetics of hH_V1 is much slower than that of many voltage-gated channels; removing Trp eliminates this distinctive property as well. In WT hH_V1, the activation time constant, τ_{act}, is in the range of seconds at room temperature, but it plummets into the low millisecond range in Trp^{207} mutants. Thus, in terms of both channel-opening kinetics and temperature dependence, the effect of removing Trp^{207} is like Kryptonite, turning a Super-channel into an ordinary mortal channel.

Proton selectivity

Over a wide range of pH, the WT hH_V1 appears to be perfectly selective. In a previous study, WT H_V1 appeared to lose selectivity between pH 9 and 10 (DeCoursey and Cherny, 1997); the present study extended only up to pH 9. The Trp^{207} mutants, however, lost selectivity at less extreme pH, beginning at pH_o 8 (Figs. 4, 7, E and F, and 8 B). It is unlikely that this loss of proton selectivity reflects a direct participation of Trp in the selectivity mechanism. It is well established that an Asp in the S1 helix is crucial to proton selectivity (Musset et al., 2011; Smith et al., 2011). This Asp can be relocated from position 112 to 116 in hH_V1 without loss of proton selectivity, but charge compensation by interaction with

one or more S4 Arg appears essential (Morgan et al., 2013). Recently, quantum mechanical calculations demonstrated an explicit mechanism by which Asp–Arg interaction is sufficient to produce proton-selective conduction without requiring contribution from the rest of the protein beyond providing a scaffold and focusing aqueous access to the selectivity filter (Dudev et al., 2015). If Trp helps anchor the S4 helix in the membrane, its removal may allow sufficient intramolecular movement to disrupt the Asp–Arg interaction that is critical to proton-selective conduction. That the loss of selectivity manifests only at high pH_o may reflect deprotonation of a cationic group that stabilizes the open channel.

Trp^{207} is essential for normal ΔpH-dependent gating

Perhaps the most striking consequence of Trp mutation is the weakening of ΔpH-dependent gating, a quintessential feature that provides the basis for H_V1 function in all cells. In all species, and even among all known H_V1 mutations described to date (Ramsey et al., 2010; Musset et al., 2011; DeCoursey, 2013), the g_H–V relationship shifts a roughly 40-mV/U change in ΔpH over a wide range of pH_o and pH_i. With the single exception of the dinoflagellate *K. veneficum* (Smith et al., 2011), this behavior results in H_V1 opening only when the electrochemical gradient is outwards, so that H_V1 extrudes acid. The mechanism of ΔpH-dependent gating remains one of the most elusive unsolved mysteries regarding H_V1. The first and only explicit model of ΔpH-dependent gating (but see Villalba-Galea, 2014) postulated titratable sites that were alternatively accessible to external or internal solutions (Cherny et al., 1995). A systematic attempt to identify which site(s) was (were) involved revealed no single ionizable residue whose mutation to a non-ionizable residue abolished this phenomenon (Ramsey et al., 2010). Rather than protonation of a site, interaction of protonated water with the Arg residues in the S4 helix was suggested to effect ΔpH-dependent gating (Ramsey et al., 2010). The possibility remained that multiple titratable sites are involved, an appealing idea because of the wide pH range over which the g_H–V relationship shifts according to the 40-mV rule. If one or more titratable sites are involved, the effect of pH might be expected to saturate. We demonstrate here that saturation of ΔpH-dependent gating does occur above pH 8.0 in WT hH_V1 (Fig. 3), consistent with previous observations in native rat proton currents (Cherny et al., 1995). Correspondingly, the regulatory sites proposed in our model were assigned a pK_a of 8.5, which was assumed to be same for access from internal or external solutions (Cherny et al., 1995).

Although distinct ΔpH-dependent gating persists in hH_V1 Trp^{207} mutants, the pH at which saturation occurred dropped to pH_o 7 but did not change for pH_i. Evidently, mutation of Trp^{207} lowers the apparent pK_a of the putative external site(s) without changing internal pH sensing. Despite not being titratable itself, Trp is evidently a key component in this mechanism, and may regulate the accessibility of another pH-sensing site, evidently increasing its effective pK_a. Because the same kind of pK_a shift occurs in both kH_V1 and hH_V1, the putative titratable group(s) may be conserved in these species. In the closed mH_V1 crystal structure (Takeshita et al., 2014) Arg^{207} (R3) is twisted away from the pore into a hydrophobic pocket of the protein. If R3 is directed away from the aqueous pore, its pK_a may be decreased substantially (Kim et al., 2005) and could thus be a candidate pH regulatory site. However, mutation of R3 did not eliminate ΔpH-dependent gating (Ramsey et al., 2010). Furthermore, experimental evidence indicates that Arg remains charged even inside proteins (Harms et al., 2011). Rather than viewing these effects as a change in effective pK_a, it is equally possible that mutation might alter the accessibility to protons of a site buried within the membrane electric field, by changing the effective dielectric constant in the pathway or the voltage drop to reach the site.

The results of this study indicate that both external and internal pH sensing may be accomplished by titratable groups with similar effective pK_a in WT hH_V1 and in two unicellular marine species: kH_V1 and EhH_V1. Furthermore, because the Trp^{207} mutation in hH_V1 (or the Trp^{176} mutation in kH_V1) selectively lowered the apparent pK_a for external but not internal pH, there appear to be distinct internal and external pH-sensing sites. This result speaks against the idea that a single site might alternatively sense pH_o and pH_i (Cherny et al., 1995), and indicates that distinct internal and external sensors (that must nevertheless interact with each other) are involved.

The kinetics of ion channel gating is often critical to their specialized function. The activation kinetics of voltage-gated Na^+ and K^+ channels is tunable by specific residues in S2 and S4 transmembrane segments (Lacroix et al., 2013). Here, we show that the highly conserved tryptophan residue in the S4 signature sequence of H_V1 (RxWRxxR) is responsible for the characteristically slow kinetics of hH_V1. By stabilizing the closed state and optimizing ΔpH sensing, Trp fine-tunes the threshold for channel opening, which in most species is just positive to E_H. Trp thus acts as a mechanism for adjusting the ΔpH-dependent gating that is prerequisite to the functions of H_V1 in all species.

We appreciate the generous gift of the EhH_V1 construct by Alison Taylor (University of North Carolina, Chapel Hill, NC) and Colin Brownlee and Glen Wheeler (Marine Biological Association of the UK, The Laboratory, Plymouth, UK). The authors appreciate helpful discussions with Artem Ayuyan (Rush University, Chicago, IL) and Valerij Sokolov (Frumkin Institute of Physical Chemistry and Electrochemistry of the Russian Academy of Sciences, Moscow, Russia).

This work is supported by US National Science Foundation award MCB-0943362 and US National Institutes of Health (NIH) grant GM102336 (to T.E. DeCoursey and S.M.E. Smith). The content is solely the responsibility of the authors and does not necessarily represent the official views of the NIH.

The authors declare no competing financial interests.

Merritt C. Maduke served as editor.

Submitted: 11 June 2015
Accepted: 18 September 2015

Note added in proof. A recent EPR spectroscopy study of hH_V1 (Li et al. 2015. The resting state of the human proton channel dimer in a lipid bilayer. *Proc. Natl. Acad. Sci. USA.* In press) showed that the dimer interface includes the top of S1 and the lower part of S4.

REFERENCES

Burley, S.K., and G.A. Petsko. 1986. Amino-aromatic interactions in proteins. *FEBS Lett.* 203:139–143. http://dx.doi.org/10.1016/0014-5793(86)80730-X

Capasso, M., M.K. Bhamrah, T. Henley, R.S. Boyd, C. Langlais, K. Cain, D. Dinsdale, K. Pulford, M. Khan, B. Musset, et al. 2010. HVCN1 modulates BCR signal strength via regulation of BCR-dependent generation of reactive oxygen species. *Nat. Immunol.* 11:265–272. http://dx.doi.org/10.1038/ni.1843

Chamberlin, A., F. Qiu, S. Rebolledo, Y. Wang, S.Y. Noskov, and H.P. Larsson. 2014. Hydrophobic plug functions as a gate in voltage-gated proton channels. *Proc. Natl. Acad. Sci. USA.* 111:E273–E282. http://dx.doi.org/10.1073/pnas.1318018111

Cherny, V.V., V.S. Markin, and T.E. DeCoursey. 1995. The voltage-activated hydrogen ion conductance in rat alveolar epithelial cells is determined by the pH gradient. *J. Gen. Physiol.* 105:861–896. http://dx.doi.org/10.1085/jgp.105.6.861

Chester, R., and T.D. Jickells. 2012. Marine Geochemistry. Vol. Third edition. Wiley-Blackwell, Hoboken, NJ. 420 pp. http://dx.doi.org/10.1002/9781118349083

DeCoursey, T.E. 2003. Voltage-gated proton channels and other proton transfer pathways. *Physiol. Rev.* 83:475–579. http://dx.doi.org/10.1152/physrev.00028.2002

DeCoursey, T.E. 2010. Voltage-gated proton channels find their dream job managing the respiratory burst in phagocytes. *Physiology (Bethesda).* 25:27–40. http://dx.doi.org/10.1152/physiol.00039.2009

DeCoursey, T.E. 2013. Voltage-gated proton channels: molecular biology, physiology, and pathophysiology of the H_V family. *Physiol. Rev.* 93:599–652. http://dx.doi.org/10.1152/physrev.00011.2012

DeCoursey, T.E., and V.V. Cherny. 1997. Deuterium isotope effects on permeation and gating of proton channels in rat alveolar epithelium. *J. Gen. Physiol.* 109:415–434. http://dx.doi.org/10.1085/jgp.109.4.415

DeCoursey, T.E., and V.V. Cherny. 1998. Temperature dependence of voltage-gated H^+ currents in human neutrophils, rat alveolar epithelial cells, and mammalian phagocytes. *J. Gen. Physiol.* 112:503–522. http://dx.doi.org/10.1085/jgp.112.4.503

DeCoursey, T.E., and E. Ligeti. 2005. Regulation and termination of NADPH oxidase activity. *Cell. Mol. Life Sci.* 62:2173–2193. http://dx.doi.org/10.1007/s00018-005-5177-1

DeCoursey, T.E., D. Morgan, and V.V. Cherny. 2003. The voltage dependence of NADPH oxidase reveals why phagocytes need proton channels. *Nature.* 422:531–534. http://dx.doi.org/10.1038/nature01523

Dudev, T., B. Musset, D. Morgan, V.V. Cherny, S.M.E. Smith, K. Mazmanian, T.E. DeCoursey, and C. Lim. 2015. Selectivity mechanism of the voltage-gated proton channel, H_V1. *Sci Rep.* 5:10320. http://dx.doi.org/10.1038/srep10320

Fischer, H. 2012. Function of proton channels in lung epithelia. *Wiley Interdiscip Rev Membr Transp Signal.* 1:247–258. http://dx.doi.org/10.1002/wmts.17

Fogel, M., and J.W. Hastings. 1972. Bioluminescence: mechanism and mode of control of scintillon activity. *Proc. Natl. Acad. Sci. USA.* 69:690–693. http://dx.doi.org/10.1073/pnas.69.3.690

Fujiwara, Y., T. Kurokawa, K. Takeshita, M. Kobayashi, Y. Okochi, A. Nakagawa, and Y. Okamura. 2012. The cytoplasmic coiled-coil mediates cooperative gating temperature sensitivity in the voltage-gated H^+ channel Hv1. *Nat. Commun.* 3:816. http://dx.doi.org/10.1038/ncomms1823

Gallivan, J.P., and D.A. Dougherty. 1999. Cation-π interactions in structural biology. *Proc. Natl. Acad. Sci. USA.* 96:9459–9464. http://dx.doi.org/10.1073/pnas.96.17.9459

Harms, M.J., J.L. Schlessman, G.R. Sue, and B. García-Moreno. 2011. Arginine residues at internal positions in a protein are always charged. *Proc. Natl. Acad. Sci. USA.* 108:18954–18959. http://dx.doi.org/10.1073/pnas.1104808108

Henderson, L.M., J.B. Chappell, and O.T.G. Jones. 1987. The superoxide-generating NADPH oxidase of human neutrophils is electrogenic and associated with an H^+ channel. *Biochem. J.* 246:325–329. http://dx.doi.org/10.1042/bj2460325

Hondares, E., M.A. Brown, B. Musset, D. Morgan, V.V. Cherny, C. Taubert, M.K. Bhamrah, D. Coe, F. Marelli-Berg, J.G. Gribben, et al. 2014. Enhanced activation of an amino-terminally truncated isoform of the voltage-gated proton channel HVCN1 enriched in malignant B cells. *Proc. Natl. Acad. Sci. USA.* 111:18078–18083. http://dx.doi.org/10.1073/pnas.1411390111

Iovannisci, D., B. Illek, and H. Fischer. 2010. Function of the HVCN1 proton channel in airway epithelia and a naturally occurring mutation, M91T. *J. Gen. Physiol.* 136:35–46. http://dx.doi.org/10.1085/jgp.200910379

Killian, J.A., and G. von Heijne. 2000. How proteins adapt to a membrane-water interface. *Trends Biochem. Sci.* 25:429–434. http://dx.doi.org/10.1016/S0968-0004(00)01626-1

Kim, J., J. Mao, and M.R. Gunner. 2005. Are acidic and basic groups in buried proteins predicted to be ionized? *J. Mol. Biol.* 348:1283–1298. http://dx.doi.org/10.1016/j.jmb.2005.03.051

Koch, H.P., T. Kurokawa, Y. Okochi, M. Sasaki, Y. Okamura, and H.P. Larsson. 2008. Multimeric nature of voltage-gated proton channels. *Proc. Natl. Acad. Sci. USA.* 105:9111–9116. http://dx.doi.org/10.1073/pnas.0801553105

Kulleperuma, K., S.M.E. Smith, D. Morgan, B. Musset, J. Holyoake, N. Chakrabarti, V.V. Cherny, T.E. DeCoursey, and R. Pomès. 2013. Construction and validation of a homology model of the human voltage-gated proton channel hH_V1. *J. Gen. Physiol.* 141:445–465.

Kuno, M., H. Ando, H. Morihata, H. Sakai, H. Mori, M. Sawada, and S. Oiki. 2009. Temperature dependence of proton permeation through a voltage-gated proton channel. *J. Gen. Physiol.* 134:191–205. http://dx.doi.org/10.1085/jgp.200910213

Lacroix, J.J., F.V. Campos, L. Frezza, and F. Bezanilla. 2013. Molecular bases for the asynchronous activation of sodium and potassium channels required for nerve impulse generation. *Neuron.* 79:651–657. http://dx.doi.org/10.1016/j.neuron.2013.05.036

Lee, S.Y., J.A. Letts, and R. Mackinnon. 2008. Dimeric subunit stoichiometry of the human voltage-dependent proton channel Hv1. *Proc. Natl. Acad. Sci. USA.* 105:7692–7695. http://dx.doi.org/10.1073/pnas.0803277105

Li, Q., S. Wanderling, M. Paduch, D. Medovoy, A. Singharoy, R. McGreevy, C.A. Villalba-Galea, R.E. Hulse, B. Roux, K. Schulten, et al. 2014. Structural mechanism of voltage-dependent gating in an isolated voltage-sensing domain. *Nat. Struct. Mol. Biol.* 21:244–252. http://dx.doi.org/10.1038/nsmb.2768

Lishko, P.V., I.L. Botchkina, A. Fedorenko, and Y. Kirichok. 2010. Acid extrusion from human spermatozoa is mediated by flagellar

voltage-gated proton channel. *Cell.* 140:327–337. http://dx.doi.org/10.1016/j.cell.2009.12.053

MacCallum, J.L., W.F.D. Bennett, and D.P. Tieleman. 2008. Distribution of amino acids in a lipid bilayer from computer simulations. *Biophys. J.* 94:3393–3404. http://dx.doi.org/10.1529/biophysj.107.112805

Morgan, D., and T.E. DeCoursey. 2014. Analysis of electrophysiological properties and responses of neutrophils. *Methods Mol. Biol.* 1124:121–158. http://dx.doi.org/10.1007/978-1-62703-845-4_9

Morgan, D., M. Capasso, B. Musset, V.V. Cherny, E. Ríos, M.J.S. Dyer, and T.E. DeCoursey. 2009. Voltage-gated proton channels maintain pH in human neutrophils during phagocytosis. *Proc. Natl. Acad. Sci. USA.* 106:18022–18027. http://dx.doi.org/10.1073/pnas.0905565106

Morgan, D., B. Musset, K. Kulleperuma, S.M.E. Smith, S. Rajan, V.V. Cherny, R. Pomès, and T.E. DeCoursey. 2013. Peregrination of the selectivity filter delineates the pore of the human voltage-gated proton channel hH_V1. *J. Gen. Physiol.* 142:625–640. http://dx.doi.org/10.1085/jgp.201311045

Musset, B., V.V. Cherny, D. Morgan, Y. Okamura, I.S. Ramsey, D.E. Clapham, and T.E. DeCoursey. 2008a. Detailed comparison of expressed and native voltage-gated proton channel currents. *J. Physiol.* 586:2477–2486. http://dx.doi.org/10.1113/jphysiol.2007.149427

Musset, B., D. Morgan, V.V. Cherny, D.W. MacGlashan Jr., L.L. Thomas, E. Ríos, and T.E. DeCoursey. 2008b. A pH-stabilizing role of voltage-gated proton channels in IgE-mediated activation of human basophils. *Proc. Natl. Acad. Sci. USA.* 105:11020–11025. http://dx.doi.org/10.1073/pnas.0800886105

Musset, B., S.M.E. Smith, S. Rajan, V.V. Cherny, D. Morgan, and T.E. DeCoursey. 2010. Oligomerization of the voltage-gated proton channel. *Channels (Austin).* 4:260–265. http://dx.doi.org/10.4161/chan.4.4.12789

Musset, B., S.M.E. Smith, S. Rajan, D. Morgan, V.V. Cherny, and T.E. DeCoursey. 2011. Aspartate 112 is the selectivity filter of the human voltage-gated proton channel. *Nature.* 480:273–277. http://dx.doi.org/10.1038/nature10557

Musset, B., R.A. Clark, T.E. DeCoursey, G.L. Petheo, M. Geiszt, Y. Chen, J.E. Cornell, C.A. Eddy, R.G. Brzyski, and A. El Jamali. 2012. NOX5 in human spermatozoa: expression, function, and regulation. *J. Biol. Chem.* 287:9376–9388. http://dx.doi.org/10.1074/jbc.M111.314955

Papazian, D.M., X.M. Shao, S.A. Seoh, A.F. Mock, Y. Huang, and D.H. Wainstock. 1995. Electrostatic interactions of S4 voltage sensor in Shaker K^+ channel. *Neuron.* 14:1293–1301. http://dx.doi.org/10.1016/0896-6273(95)90276-7

Pettersen, E.F., T.D. Goddard, C.C. Huang, G.S. Couch, D.M. Greenblatt, E.C. Meng, and T.E. Ferrin. 2004. UCSF Chimera—a visualization system for exploratory research and analysis. *J. Comput. Chem.* 25:1605–1612. http://dx.doi.org/10.1002/jcc.20084

Ramsey, I.S., M.M. Moran, J.A. Chong, and D.E. Clapham. 2006. A voltage-gated proton-selective channel lacking the pore domain. *Nature.* 440:1213–1216. http://dx.doi.org/10.1038/nature04700

Ramsey, I.S., Y. Mokrab, I. Carvacho, Z.A. Sands, M.S.P. Sansom, and D.E. Clapham. 2010. An aqueous H^+ permeation pathway in the voltage-gated proton channel Hv1. *Nat. Struct. Mol. Biol.* 17:869–875. http://dx.doi.org/10.1038/nsmb.1826

Roos, A., and W.F. Boron. 1981. Intracellular pH. *Physiol. Rev.* 61:296–434.

Santiveri, C.M., and M.A. Jiménez. 2010. Tryptophan residues: scarce in proteins but strong stabilizers of β-hairpin peptides. *Biopolymers.* 94:779–790. http://dx.doi.org/10.1002/bip.21436

Smith, S.M.E., D. Morgan, B. Musset, V.V. Cherny, A.R. Place, J.W. Hastings, and T.E. DeCoursey. 2011. Voltage-gated proton channel in a dinoflagellate. *Proc. Natl. Acad. Sci. USA.* 108:18162–18167. http://dx.doi.org/10.1073/pnas.1115405108

Takeshita, K., S. Sakata, E. Yamashita, Y. Fujiwara, A. Kawanabe, T. Kurokawa, Y. Okochi, M. Matsuda, H. Narita, Y. Okamura, and A. Nakagawa. 2014. X-ray crystal structure of voltage-gated proton channel. *Nat. Struct. Mol. Biol.* 21:352–357. http://dx.doi.org/10.1038/nsmb.2783

Tatko, C.D., and M.L. Waters. 2003. The geometry and efficacy of cation-π interactions in a diagonal position of a designed β-hairpin. *Protein Sci.* 12:2443–2452. http://dx.doi.org/10.1110/ps.03284003

Taylor, A.R., A. Chrachri, G. Wheeler, H. Goddard, and C. Brownlee. 2011. A voltage-gated H^+ channel underlying pH homeostasis in calcifying coccolithophores. *PLoS Biol.* 9:e1001085. http://dx.doi.org/10.1371/journal.pbio.1001085

Tombola, F., M.H. Ulbrich, and E.Y. Isacoff. 2008. The voltage-gated proton channel Hv1 has two pores, each controlled by one voltage sensor. *Neuron.* 58:546–556. http://dx.doi.org/10.1016/j.neuron.2008.03.026

Villalba-Galea, C.A. 2014. Hv1 proton channel opening is preceded by a voltage-independent transition. *Biophys. J.* 107:1564–1572. http://dx.doi.org/10.1016/j.bpj.2014.08.017

Wang, Y., S.J. Li, X. Wu, Y. Che, and Q. Li. 2012. Clinicopathological and biological significance of human voltage-gated proton channel Hv1 protein overexpression in breast cancer. *J. Biol. Chem.* 287:13877–13888. http://dx.doi.org/10.1074/jbc.M112.345280

Wood, M.L., E.V. Schow, J.A. Freites, S.H. White, F. Tombola, and D.J. Tobias. 2012. Water wires in atomistic models of the Hv1 proton channel. *Biochim. Biophys. Acta.* 1818:286–293. http://dx.doi.org/10.1016/j.bbamem.2011.07.045

Wu, L.J., G. Wu, M.R. Akhavan Sharif, A. Baker, Y. Jia, F.H. Fahey, H.R. Luo, E.P. Feener, and D.E. Clapham. 2012. The voltage-gated proton channel Hv1 enhances brain damage from ischemic stroke. *Nat. Neurosci.* 15:565–573. http://dx.doi.org/10.1038/nn.3059